

Coordinated Resource Scheduling in a Large Scale Virtual Power Plant Considering Demand Response and Energy Storages

H. M. Samakoosh¹, M. Jafari-Nokandi^{2,*}, A. Sheikholeslami²

¹Mazandaran University of Science and Technology, Babol, Iran.

²Department of Electrical and Computer Engineering, Babol Noshirvani University of Technology, Babol, Iran.

Abstract- Virtual power plant (VPP) is an effective approach to aggregate distributed generation resources under a central control. This paper introduces a mixed-integer linear programming model for optimal scheduling of the internal resources of a large scale VPP in order to maximize its profit. The proposed model studies the effect of a demand response (DR) program on the scheduling of the VPP. The profit of the VPP is calculated considering different components including the income from the sale of electricity to the network and the incentives received by the renewable resources, fuel cost, the expense of the purchase of electricity from the network and the load curtailment cost during the scheduling horizon. The proposed model is implemented in a large scale VPP that consists of five plants in two cases: with and without the presence of the DR. Simulation results show that the implementation of the DR program reduces the operation cost in the VPP, therefore increasing its profit.

Keyword: Virtual power plant, Demand response, Distributed energy resources, storage, Mixed-integer linear programming.

Sets and indices

n	Index for load profile
R	Index for region
s	Index for customer
t, τ	Index for time period

Parameters

$f_{max,R}$	Maximum capacity of line R
IP_{pv}	Incentive price for solar power
IP_w	Incentive price for wind power
$IV_{ES-initial,R}$	Initial energy level of electrical storage in region R
$IV_{ES-min,R}$	Minimum energy level of electrical storage in region R
$IV_{ES-max,R}$	Maximum energy level of electrical storage in region R
$IV_{TS-initial,R}$	Initial energy level of thermal storage in region R
$IV_{TS-min,R}$	Minimum energy level of thermal storage in region R
$IV_{TS-max,R}$	Maximum energy level of thermal storage in region R
$L_{prof,s,n,t}$	Demand of customer s at time t according to the n th load profile
m	Penalty factor for deselecting the main load

	profiles
N_R	Number of customers in region R
$N_{s,R}$	Total number of load profiles declared by customer s in region R
$P_{boil-max,R}$	Maximum power of boiler in region R
$P_{echp-min,R}$	Minimum power of CHP in region R
$P_{echp-max,R}$	Maximum power of CHP in region R
$P_{ES-ch,R}$	Maximum charge power of electrical storage in region R
$P_{ES-disc,R}$	Maximum discharge power of electrical storage in region R
$P_{pv-max,R}$	Maximum power output of photovoltaic cells in region R , at time t
$P_{TS-ch,R}$	Maximum charge power of thermal storage in region R
$P_{TS-disc,R}$	Maximum discharge power of thermal storage in region R
$P_{w-max,R}$	Maximum power output of wind turbines in region R , at time t
$q_{s,n,R}$	Rank of the n th load profile of customer s in region R
T	Number of periods in the scheduling horizon
$TL_{R,t}$	Thermal load of region R , at time t
$VOLL$	Value of lost load
$\pi_{pp,t}$	Electricity purchase price at time t
$\pi_{sp,t}$	Electricity sale price at time t
Φ_R	Generation cost of boiler in region R
φ_R	Generation cost of CHP in region R
$\lambda_{chp,R}$	Heat to electrical ratio of CHP in region R
$\eta_{ES,R}$	Charging efficiency of electrical storage in region R
$\eta_{TS,R}$	Charging efficiency of thermal storage in

Received: 25 Dec. 2016

Revised: 12 Aug. 2017

Accepted: 15 Sep. 2017

*Corresponding author:

E-mail: m.jafari@nit.ac.ir (M. Jafari-Nokandi)

Digital object identifier: 10.22098/joape.2018.3153.1257

	region R
$\gamma_{EL,R}$	Maximum load curtailment in region R (in percent)
Variables	
a_t	Binary variable which is 1 if the VPP sells power to network at time t .
$A_{R,t}$	Charge power of electrical storage in region R , at time t
$B_{R,t}$	Discharge power of electrical storage in region R , at time t
$C_{R,t}$	Charge power of thermal storage in region R , at time t
$D_{R,t}$	Discharge power of thermal storage in region R , at time t
$C_{fuel,R,t}$	Fuel cost for boiler and CHP productions in region R , at time t
$C_{pcc,R,t}$	Cost of purchasing or income from selling electrical energy in region R , at time t
$E_{R,t}$	Power output from Region R , at time t
$EL_{R,t}$	Electrical load of region R , at time t
$f_{R,t}$	Power flow on line R from region R to region $R+1$
$F_{R,t}$	Power input to region R , at time t
$P_{boil,R,t}$	Power output of boiler in region R , at time t
$P_{curtail,R,t}$	Electrical load curtailment in region R , at time t
$P_{echp,R,t}$	Electrical power output of CHP in region R , at time t
$P_{ES,R,t}$	Power output of electrical storage in region R , at time t
$P_{int,R,t}$	Power output of region R , at time t
$P_{pv,R,t}$	Power output of photovoltaic systems in region R , at time t
$P_{surplus,R,t}$	Thermal power surplus in region R , at time t
$P_{tchp,R,t}$	Thermal power output of CHP in region R , at time t
$P_{TS,R,t}$	Power output of thermal storage in region R , at time t
$P_{w,R,t}$	Power output of wind turbines in region R , at time t
$sale_{R,t}$	Binary variable which is 1 if $P_{int,R,t}$ is positive.
$U_{s,R}$	Penalty term for deselecting the main load profile of customer s in region R
U	Total penalty for deselecting the main load profiles of customers in the VPP
$v_{i,R}$	Binary variable which is 1 if CHP unit of region R is on.
$x_{s,n,R}$	Binary variable which is 1 if load profile n is selected for customer s in region R .
$ZE_{R,t}$	Binary variable which is 1 if the electrical storage in region R is charging at time t
$ZT_{R,t}$	Binary variable which is 1 if the thermal storage in region R is charging at time t

Acronyms

CHP	Combined heat and power generation
EL	Electrical load
DG	Distributed generation

DER	Distributed energy resources
PV	Photovoltaic cells
TL	Thermal load
VPP	Virtual power plant
WT	Wind turbines

1. INTRODUCTION

Nowadays, financial constrictions and environmental concerns have led to the utilization of renewable energy resources in a decentralized generation framework instead of conventional power plants [1]. As the role of distributed generations is increasing in distribution networks, their negative aspects impose new challenges on future power systems, including the low capacity of individual DGs which hinders their participation in electricity markets. Aggregating distributed energy resources (DER) is an effective way to eliminate this issue. Therefore, virtual power plant (VPP) has been introduced as an important feature of smart grids. VPP can be defined as a set of loads, DGs, and storages that are aggregated to achieve a higher production capacity [2], [3]. Integrating different DERs within VPPs can be an effective way to abate emissions, operational expenses and technical challenges of electric distribution networks [4]. Moreover, a VPP can integrate DERs as a single market agent. This means that unlike a small micro grid that only supplies local loads, VPPs have the potential to participate in the wholesale energy market or provide ancillary services [5]. Consequently, an important matter concerning VPPs is the optimal scheduling of their internal resources in order to carry out the above tasks efficiently [6].

A number of bidding strategies for VPPs have been proposed to participate in the electricity markets in literature. In [3], the participation of a VPP in the day-ahead market and the balancing market has been considered using a stochastic programming approach. The uncertainties involved in the electricity price, the generation of renewable resources and the consumption of loads have been taken into account. The bidding strategy problem is formulated in [7] as a two-stage programming model that maximizes the VPP expected profit. In [8] and [9], a price-based unit commitment method has been proposed as an appropriate solution for the bidding strategy of the VPP in the energy market. However, the authors have not considered the presence of renewable energy sources and demand response programs. A modified particle swarm optimization approach has been presented in [10] to minimize the day-ahead cost of VPP. In [11], the optimal thermal and electrical scheduling of a large scale VPP including energy storages is introduced in order to maximize its

profit in a 24-hour horizon. The algorithm takes the actual location of each DER in the public network and its specific capability into account. In [12], a stochastic model using a modified scenario-based decision making method is proposed for optimal day-ahead scheduling of electrical and thermal energy resources in a large scale VPP.

In restructured power systems, implementing DR programs is one of the most important approaches to enable the system operator to control its subset loads. It also increases the competition in the electricity market as well as improving network reliability [13]. According to a survey of Federal Energy Regulatory Commission (FERC), the implementation of DR programs was reported to have significant effects on system and market operation, such as increases in network reliability and reductions in energy cost and the customer's electricity bills by 52%, 30% and 36% in 2005 [14]. Thus, VPP operators can utilize DR as a tool to control the local load and reduce the total cost of the VPP while increasing its profit.

A DR model is developed in [15] which offers optimal levels for both production and consumption in a smart grid consisting of a wind farm along with conventional resources. In [16-18], DR programs are defined based on the time-of-use (TOU) pricing mechanism and interruptible loads. In [19], an optimal model for the dynamic economic emission dispatch problem in the presence of the emergency demand response program has been developed. In [20], a novel concept of smart distribution system expansion planning is presented which expands the concept of demand response programs to be dealt with in the long-term horizon time. The proposed framework integrates demand response resources into the distribution expansion planning as virtual distributed generation resources. In [21], renewable energy resources are aggregated and controlled by an energy management system in order to operate as a VPP and participates as a VPP in a day-ahead DR program to relieve network congestion and improve market efficiency. In [22], exploiting the DR exchange market for efficient energy management of a VPP with significant penetration of wind energy is proposed. Numerical results have shown that employing the DR market mechanism can result in significant improvement in the VPP's profit. A novel DR scheme is proposed in [23] which eliminates the need to predict the price elasticity of demand. The scheme is performed on the submissions of candidate load profiles by consumers which are ranked in preference order. The load aggregator then performs the final selection of individual

load profiles subject to the total cost minimization.

According to literature, the majority of the pervious works on VPPs have focused on the bidding strategy of the VPP to participate in the electricity and ancillary services markets. On the other hand, the proposed model in this paper is a developed version of the model described by [11] which takes the implementation of a DR scheme into account. It investigates the effect of the DR program on the scheduling of VPP resources and its operation cost and profit. It is shown that the DR program can lead to a decrease in electrical demand at peak load hours and the operational cost of the VPP.

The rest of this paper is organized as follows: Section 2 describes the proposed VPP structure and the problem assumptions. Section 3 delves into the mathematical formulation of the DR program and the VPP scheduling problem. Section 4 illustrates the simulation results, and finally, a conclusion is presented in Section 5.

2. THE STRUCTURE OF THE LARGE SCALE VPP

As shown in Fig. 1, a large scale VPP consisting of a number of regions or plants that are distributed over a relatively large geographic area is considered in this study [11]. Each area includes a number of customers with the corresponding electrical and thermal load. According to Fig. 2, each area can include a combined heat and power generation (CHP) unit, a thermal generator (boiler) and electrical and thermal storages. It can also include distributed generation resources such as photovoltaic cells (PV) and wind turbines.

The VPP operator is responsible for providing electrical and thermal energy for local loads with the consideration of network security constraints. For this purpose, the generation resources within the VPP are scheduled based on the production cost considering technical constraints and transmission line limitations. The local thermal load can be supplied by the CHP unit, the boiler or the thermal storage. The over-produced thermal and electrical energy of each plant can either be stored in the corresponding storages or be sold to the network. On the other hand, shortages in generation can either be compensated by the stored energy or be purchased from the network. If it is not possible to supply the electricity demand due to the network constraints or inadequacy of generation resources, the load should be curtailed. It is also assumed that the electrical loads can participate in the DR program. The goal of the VPP is to maximize profit through scheduling the internal resources and managing the load profiles of the DR

providers.

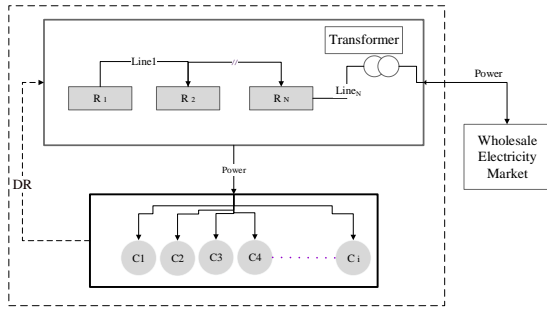


Fig. 1 The structure of the large scale VPP including demand response

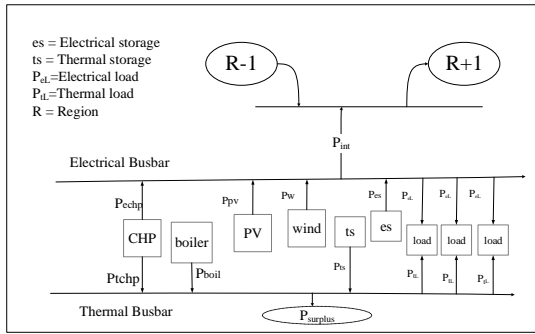


Fig. 2. The components of each region of the VPP

3. MODEL FORMULATION

3.1. Demand response model

In this work, the proposed concept in [23] is used to implement the DR program. It is assumed that each customer participating in the DR program submits a daily load profile, namely the main load profile, and a number of alternative load profiles according to their priority. The VPP operator selects one load profile for each customer to maximize the VPP daily profit. Assuming that customer s in region R declares $N_{s,R}$ load profiles including the main one and the alternatives, the rank of the n th load profile is defined as follows:

$$q_{s,n,R} = n - 1 \tag{1}$$

In order to determine the selected load profiles, the binary variable $x_{s,n,R}$ is introduced which equals 1 if the n th load profile is chosen for the customer s in region R . According to Eq. (2), only one load profile will be selected for each customer:

$$\sum_{n=1}^{N_{s,R}} x_{s,n,R} = 1 \tag{2}$$

Considering the selected load profiles, the hourly electrical load of region R is calculated as follows:

$$EL_{R,t} = \sum_{s=1}^{N_R} x_{s,n,R} L_{prof.s,n,t} \tag{3}$$

where N_R is the number of customers in region R and $L_{prof.s,n,t}$ is the hourly load of customer s corresponding to the n th load profile. To respect the priority of load profiles, the selection of those with lower ranks is penalized as follows:

$$U_{s,R} = \sum_{t=1}^T \sum_{n=1}^{N_{s,R}} q_{s,n} x_{s,n} L_{prof.s,n,t} \pi_{pp,t} \tag{4}$$

where $U_{s,R}$ is the penalty term corresponding to deselecting the main load profile of customer s in region R , and $\pi_{pp,t}$ is the electricity purchase price at time t . If the VPP consists of N regions, the total penalty for deselecting the main load profiles during period T is calculated as follows:

$$U = m \sum_{R=1}^N \sum_{s=1}^{N_R} U_{s,R} \tag{5}$$

where m is the penalty factor for deselecting the main load profiles.

3.2. Optimal scheduling of VPP resources

In order to maximize the net profit of the VPP, the scheduling of the DER and load profiles is performed. The objective function of the optimization model is

$$Max(net) = \left(\sum_{t=1}^T \sum_{R=1}^N C_{pcc,R,t} + IP_w P_{w,R,t} + IP_{pv} P_{pv,R,t} - C_{fuel,R,t} - VOLL P_{curtail,R,t} \right) - U \tag{6}$$

where $C_{pcc,R,t}$ is the income from power interchange between region R and the grid at time t determined according to the purchase or sale of electrical energy; IP_w and IP_{pv} are the incentive prices for the wind and solar powers; $P_{w,R,t}$ and $P_{pv,R,t}$ are the power production of wind turbines and the photovoltaic system in region R at time t ; $P_{curtail,R,t}$ is the electrical load curtailment in region R at time t , and $VOLL$ is the value of the lost load.

The first term in the objective functions is the revenue from selling electricity to the market when power is delivered to the grid. This term is negative when power is received from the grid and represents the cost of purchasing electricity from the network. The second and third terms are the revenue from the incentives received by wind and photovoltaic power, respectively. The fourth term expresses the fuel cost required for the generation of thermal power and electricity by the boiler and CHP. The fifth term is the load curtailment cost, and the last is the penalty corresponding to deselecting the first load profile of the DR providers. If customers do not participate in the

DR program, the last term in the objective function is ignored and the main load profiles are selected for all customers. It should be noted that the last term in the objective function is not a real cost and is considered only to respect the priority of load profiles. Therefore, after scheduling the VPP, the real profit is calculated as follows:

$$\text{True profit} = \text{net} + U \quad (7)$$

The cost of purchasing or selling electrical energy is computed by the following equation:

$$\begin{cases} C_{pcc.R,t} = \pi_{pp,t} P_{int.R,t} & \text{if } P_{int.R,t} < 0 \\ C_{pcc.R,t} = \pi_{sp,t} P_{int.R,t} & \text{if } P_{int.R,t} > 0 \end{cases} \quad (8)$$

where $\pi_{sp,t}$ is the hourly electricity sale price and $P_{int,R,t}$ is the power output of the region R at time t .

The fuel cost of the boiler and CHP is calculated as follows:

$$C_{fuel.R,t} = \phi_R p_{boil.R,t} + \varphi_R p_{echp.R,t} \quad (9)$$

where ϕ_R and φ_R are the power generation cost of the boiler and CHP in region R , respectively, and $P_{boil,R,t}$ and $P_{echp,R,t}$ are the power output of the boiler and CHP in region R at time t .

The objective function should be optimized owing to the following constraints.

$$P_{int.R,t} = p_{echp.R,t} + P_{pv.R,t} + P_{w.R,t} + P_{ES.R,t} + P_{curtail.R,t} - EL_{R,t} \quad (10)$$

$$p_{tchp.R,t} + p_{boil.R,t} + P_{TS.R,t} = TL_{R,t} + P_{surplus.R,t} \quad (11)$$

$$P_{surplus.R,t} \geq 0 \quad (12)$$

where $P_{ES,R,t}$ and $P_{TS,R,t}$ are the hourly power output of electrical and thermal storages in region R ; $P_{tchp,R,t}$ is the thermal power output of the CHP in region R at time t ; $TL_{R,t}$ is the thermal load of region R at time t and $P_{surplus,R,t}$ is the thermal power surplus in region R at time t . The electrical and thermal power balance equations for each region of the VPP are presented by Eqs. (10) and (11). The thermal power cannot be transmitted between the regions. Therefore, the excessive thermal power of each region should be saved in its own thermal storage, or otherwise be dissipated as $P_{surplus,R,t}$ according to Eqs. (11) and (12).

Equation (13) illustrates that the electrical power generation of the CHP unit should be within its minimum and maximum generation capacity. Equation (14) expresses the thermal power generation ratio to the electrical power of the CHP unit. Equations (15) to (17) state the limitations of the thermal power of the boilers

and the electrical power of wind turbines and photovoltaic systems, respectively. Equation (18) determines the power flow on the lines between the regions, while Eq. (19) indicates that the power flow is limited to the line capacity. The equations are presented as follows:

$$v_{t,R} p_{echp-min,R} \leq p_{echp.R,t} \leq v_{t,R} p_{echp-max,R} \quad (13)$$

$$p_{tchp.R,t} = \lambda_{chp} p_{echp.R,t} \quad (14)$$

$$0 \leq p_{boil.R,t} \leq p_{boil-max,R} \quad (15)$$

$$0 \leq P_{pv.R,t} \leq P_{pv-max,R} \quad (16)$$

$$0 \leq P_{w.R,t} \leq P_{w-max,R} \quad (17)$$

$$f_{R,t} = P_{int.R,t} + f_{R-1,t} \quad (18)$$

$$-f_{max,R} \leq f_{R,t} \leq f_{max,R} \quad (19)$$

where $v_{t,R}$ is a binary variable which is 1 if the CHP unit of region R is on; $P_{echp-min,R}$ and $P_{echp-max,R}$ are the minimum and maximum generation capacity of the CHP unit in region R ; $P_{boil-max,R}$ is the maximum power of the boiler in region R ; λ_{chp} is the heat to electrical ratio of the CHP unit; $P_{pv-max,R}$ and $P_{w-max,R}$ are the maximum power output of the photovoltaic system and wind turbines in region R at time t ; $f_{R,t}$ is the power flow on line R from region R to region $R+1$, and $f_{max,R}$ is the maximum capacity of line R .

Equations (20) and (21) indicate the maximum power during the charging and discharging operation for electrical and thermal storages. Equations (22) and (23) express the constraints of the electrical and thermal energy storage capacities. Equations (24) and (25) guarantee that the initial energy level of the storages will be recovered at the end of the scheduling horizon. If it is not possible or economical to meet the whole electricity demand of the VPP due to line limits or the high price of electricity, load curtailment is scheduled for each region up to a maximum ratio of $\gamma_{EL,R}$ according to Equation (26). The linearized forms of Eqs. (8), (22) and (23) are presented in appendix A.

$$-P_{ES-ch,R} \leq P_{ES.R,t} \leq P_{ES-disc,R} \quad (20)$$

$$-P_{TS-ch,R} \leq P_{TS.R,t} \leq P_{TS-disc,R} \quad (21)$$

$$\begin{aligned} IV_{ES-initial,R} - IV_{ES-max,R} \leq \\ \eta_{ES,R} \sum_{\tau=1}^t \underset{\text{charging}}{P_{ES.R,\tau}} + \sum_{\tau=1}^t \underset{\text{discharging}}{P_{ES.R,\tau}} \\ \leq IV_{ES-initial,R} - IV_{ES-min,R} \end{aligned} \quad (22)$$

$$IV_{TS-initial,R} - IV_{TS-max,R} \leq \eta_{TS,R} \sum_{\tau=1}^t P_{TS,R,\tau} + \sum_{\tau=1}^t P_{TS,R,\tau} \quad (23)$$

$$\leq IV_{TS-initial,R} - IV_{TS-min,R}$$

$$\eta_{ES,R} \sum_{t=1}^T P_{ES,R,t} + \sum_{t=1}^T P_{ES,R,t} = 0 \quad (24)$$

$$\eta_{TS,R} \sum_{t=1}^T P_{TS,R,t} + \sum_{t=1}^T P_{TS,R,t} = 0 \quad (25)$$

$$P_{curtail,R,t} \leq \gamma_{EL,R} E_{L,R,t} \quad (26)$$

where $P_{ES-ch,R}$ and $P_{ES-disc,R}$ are the maximum charge and discharge power of the electrical storage in region R , respectively; $P_{TS-ch,R}$ and $P_{TS-disc,R}$ are the maximum charge and discharge power of the thermal storage in region R ; $\eta_{ES,R}$ and $\eta_{TS,R}$ are the charging efficiency of the electrical and thermal storages in region R ; $IV_{ES-initial,R}$ and $IV_{TS-initial,R}$ are the initial energy level of the electrical and thermal storages in region R ; $IV_{ES-min,R}$ and $IV_{ES-max,R}$ are the minimum and maximum energy capacity of the electrical storages in region R ; $IV_{TS-min,R}$ and $IV_{TS-max,R}$ are the minimum and maximum energy capacity of the thermal storage in region R , respectively, and $\gamma_{EL,R}$ is the maximum load curtailment in region R in percent.

According to the results of the optimization model, the hourly values of the cost, the revenue and the profit of the VPP can be calculated as follows:

$$\text{cost}_t = \sum_{R=1}^N C_{fuel,R,t} + VOLL P_{curtail,R,t} \quad (27)$$

$$-(1 - a_t) \pi_{pp,t} P_{int,R,t}$$

$$\text{Revenue}_t = \sum_{R=1}^N a_t \pi_{sp,t} P_{int,R,t} + IP_w P_{w,R,t} + IP_{pv} P_{pv,R,t} \quad (28)$$

$$\text{profit}_t = \text{Revenue}_t - \text{cost}_t \quad (29)$$

where a_t is a binary variable which is 1 if the VPP sells power to the network and 0 otherwise.

4. SIMULATION RESULTS

The proposed model for the scheduling of the VPP has been implemented in a distribution network including five regions. Table 1 shows the data of the VPP equipment [11]. Table 2 presents the purchase and sale prices of the electricity, the hourly thermal loads and the

forecasted generation of the photovoltaic system and wind turbines at each region [11]. The information of the alternative load profiles of the customers are extracted from NIYSO [24] with some modifications which are shown in Appendix B. The VOLL is assumed to be 8 euro/kWh and the incentive payments to the photovoltaic and wind generations are assumed 0.3 and 0.4 euro/kWh, respectively [11]. The simulations are carried out in GAMS environment using the CPLEX 12.5.1.0 solver.

The proposed scheduling model is investigated in two scenarios:

- Scenario 1: scheduling of the VPP without the participation of customers in the DR program
- Scenario 2: scheduling of the VPP with the implementation of the DR program

In the first scenario, customer demands are equal to their main load profiles. Therefore, the VPP supplies the demands solely through its internal resources or purchase from the electricity market. In this case, the total profit for the VPP will be -554.6 euro.

On the other hand, in the second scenario where the DR program is implemented, the VPP operator can select one load profile among the declared alternatives for each customer. The penalty factor for deselecting the first load profile is considered to be $m=0.01$.

Table 1. Data of the components of the VPP

Parameter	unit	Region1	Region2	Region3	Region4	Region5
$P_{chp-min}$	kW	5	10	20	55	20
$P_{chp-max}$	kW	50	80	100	90	150
λ_{chp}	-	1.5	0.7	1.1	0.9	1
$P_{ES-ch,R}$	kW	7	5	1	10	1
$P_{ES-disc,R}$	kW	7	5	1	10	1
$P_{TS-ch,R}$	kW	5	10	5	5	7
$P_{TS-disc,R}$	kW	5	10	5	5	7
$P_{boil-max,R}$	kW	30	70	70	55	70
$IV_{ES-min,R}$	kWh	10	20	0	0	4
$IV_{ES-max,R}$	kWh	30	60	10	20	30
$IV_{ES-initial}$	kWh	20	50	10	40	10
$IV_{TS-min,R}$	kWh	10	10	5	0	0
$IV_{TS-max,R}$	kWh	40	70	20	40	30
$IV_{TS-initial,R}$	kWh	20	50	10	40	10
$\eta_{ES,R}$	-	1	1	1	1	1
$\eta_{TS,R}$	-	1	1	1	1	1
Φ_R	-	0.45	0.40	0.43	0.45	0.41
ϕ_R	-	0.123	0.111	0.149	0.111	0.81
$f_{max,R}$	kW	500	500	75	80	500
$\gamma_{EL,R}$	-	0.1	0.1	0.1	0.1	0.1

Table 3 represents the selected load profiles for each customer. It can be seen that the 4th and the 5th load profiles have been chosen for several customers due to their lower demand levels at peak hours.

Table 2. Data of thermal load (kW), electricity prices (euro/MWh) and forecasted solar and wind power(kW) at each region [11]

Hour	Price		Region1			Region2			Region3			Region4			Region5		
	Purchase	sale	TL	P _{pv}	P _w	TL	P _{pv}	P _w	TL	P _{pv}	P _w	TL	P _{pv}	P _w	TL	P _{pv}	P _w
1	106	63	99	0	0	0	0	0	33	0	11	60	0	0	0	0	6
2	106	53	99	0	0	0	0	0	33	0	7	60	0	0	0	0	2
3	106	51	99	0	1	0	0	0	33	0	0	59	0	0	0	0	4
4	106	50	99	0	0	0	0	0	33	0	0	60	0	0	0	0	1
5	106	51	99	0	6	0	0	0	33	0	2	60	0	0	0	0	0
6	106	52	100	0	6	0	0	3	33	0	7	60	0	1	0	0	0
7	106	63	92	2	0	2	2	0	34	3	2	59	3	0	2	2	0
8	125	67	84	5	2	98	5	6	35	5	4	60	5	1	79	5	0
9	135	73	89	10	2	112	9	3	5	10	7	60	11	0	68	11	1
10	135	80	88	2	6	105	2	0	61	2	7	59	3	4	71	3	0
11	135	80	88	7	4	117	6	0	68	8	2	59	7	1	90	7	1
12	135	80	83	11	13	100	11	0	70	12	2	59	11	4	75	13	0
13	135	70	92	14	6	86	12	10	70	15	0	59	14	4	1	15	1
14	135	69	97	11	9	117	12	16	65	11	24	60	11	4	0	13	0
15	135	73	97	7	13	105	6	0	65	8	0	60	7	4	2	7	0
16	135	79	97	2	9	115	2	3	68	2	0	60	3	24	22	2	0
17	135	80	97	24	2	117	24	3	67	24	0	60	24	17	82	24	3
18	135	71	95	17	24	112	17	24	58	16	0	59	19	11	83	17	0
19	135	66	95	10	24	111	10	3	50	11	0	59	10	4	83	10	6
20	125	67	95	5	4	102	5	16	40	5	0	59	5	4	68	5	6
21	125	72	96	2	4	2	3	16	44	3	1	59	3	4	2	3	13
22	125	77	95	0	6	0	0	0	33	0	0	60	0	0	0	0	24
23	125	67	94	0	2	0	0	0	32	0	0	60	0	0	0	0	17
24	106	63	93	0	1	0	0	0	32	0	0	60	0	0	0	0	13

Therefore, the VPP operator can decrease the cost of producing or purchasing electrical energy in these periods. The total profit for the VPP will thus equal -510.8 euro, which shows 8% saving compared to the first scenario. Moreover, according to Table 3, when the penalty factor increases, the flexibility to manage the electrical demand decreases and the VPP operator selects the first load profiles for the majority of the customers. As Fig. 3 illustrates, the total electrical load of the VPP decreases when the penalty factor increases, resulting in the decrease of the VPP operation cost.

Table 3. The selected load profile considering different values for the penalty factor

Customer	Penalty Factor (m)		
	0.01	0.02	0.2
1	4	4	1
2	4	4	1
3	4	4	1
4	1	1	1
5	4	4	1
6	4	4	1
7	1	1	1
8	4	4	1
9	4	1	1
10	1	1	1
11	1	1	1
12	1	1	1
13	5	1	1
14	5	1	1
15	5	1	1

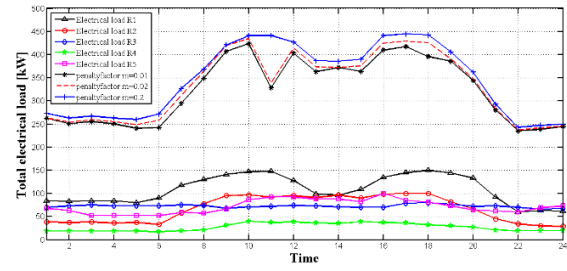


Fig. 3 the main load profiles of the regions and total electrical load of the VPP in scenario 2

Figures 4 to 8 show the scheduling results for the CHP units, the boilers, the electrical and thermal storages and the power flow on lines in the scheduling horizon in the presence of the DR program. Fig. 4 demonstrates the scheduled power production of the CHP at each plant. The CHP unit of region 1 operates at its full capacity in all hours due to the excessive thermal demand at this region. The production of the CHP unit in region 2 has the same pattern between hours 8 and 20 in which the thermal load of this region increases. It should be noted that generation of thermal power using the CHP unit is more economical in comparison to generation utilizing the boiler. Therefore, the prior resources of the VPP to supply thermal loads are the CHP units, which can supply a part of the electrical loads simultaneously. However, when compared to scenario 1, the power production of the CHP units decreases during peak load periods due to the selection of the load profiles with less consumption. Consequently, the fuel consumption of the CHP units reduces and fuel cost decreases.

Figure 5 illustrates the hourly production of the boilers. The boilers in regions 1 and 2 operate in almost all periods due to the lack of thermal power generation considering their CHP capacity. On the other hand, the CHP production of regions 3 to 5 covers the majority of their thermal loads. Therefore, the times in which the thermal power productions of the CHP units are not sufficient to meet the local thermal loads, and thus the boilers should operate, occur less frequently. In comparison to scenario 1, the boiler of region 2 increases its production in the early hours (1 AM to 5 AM) and the hours 13 and 17. This is due to the reduction of the power output of the CHP unit in these periods which results in the decrease of thermal power production.

Figure 6 shows the power flow on lines. The power flows of lines 1 and 2 are always negative, which means that the generation resources of regions 1 and 2 cannot cover the high level of electrical demand and thus receive electrical power from the neighbor regions. A significant part of this inadequacy is compensated with the purchase of electricity from the network. Therefore, the power

flow on line 3 is mostly negative, in other words, the line transfers the purchased power to these regions. Furthermore, the power flow on line 3 reaches its transmission capacity until 10 AM. The power flow on line 5 is positive between the hours 11 to 18 and 21 to 22 when the sale price of electricity is higher. Thus, it is beneficial for the VPP to sell electricity to the network in these hours.

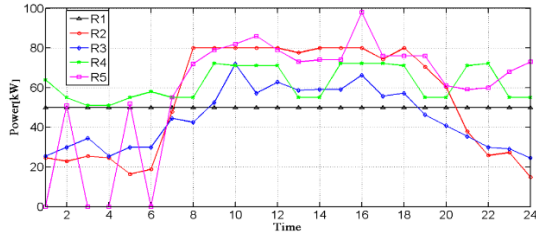


Fig. 4 Electrical power generation of the CHP units in scenario 2

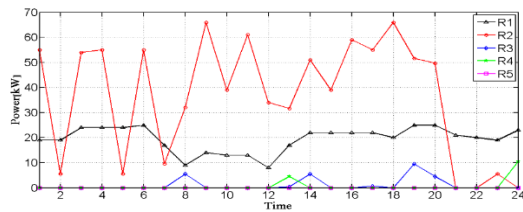


Fig. 5 Power production of the boilers in scenario 2

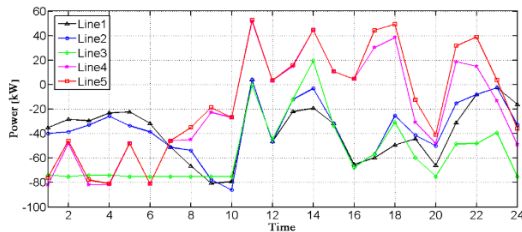


Fig. 6 Power flow on lines in scenario 2

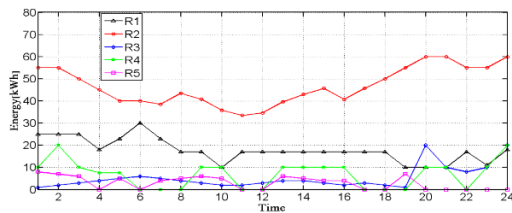


Fig. 7 state-of-charge of the electrical storages in scenario 2

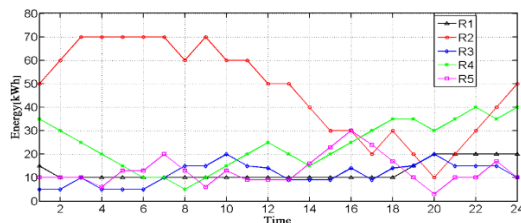
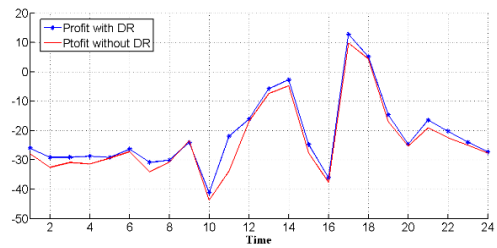


Fig. 8 state-of-charge of the thermal storages in scenario 2

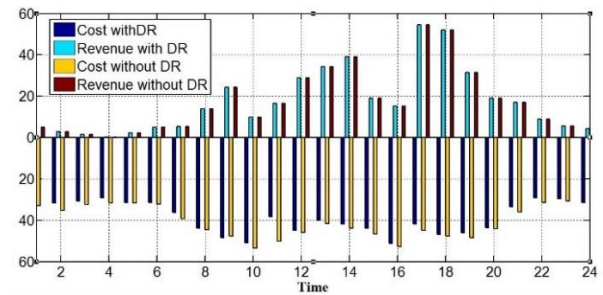
Figure 7 and Fig. 8 demonstrate the electrical and thermal energy stored in the storages, respectively. It can be seen that the stored energy level of the storages returns to its initial value at the end of the scheduling horizon. Since the power flow on line 3 reaches its capacity in the

early hours, the VPP is forced to utilize the energy stored in the electrical storage of region 2 to meet its local load and prevent load curtailment.

Figure 9 compares the hourly cost, revenue and profit of the VPP in both scenarios. With the selection of low-consumption load profiles, the VPP can provide the customers' demand at a cheaper cost. Therefore, the profit of the VPP increases in most of the hours in the presence of the DR. The maximum profits for the VPP occur in hours 17 and 18 when the sale price of electricity is high. Moreover, the profit is positive in these hours, i.e., the VPP earns money from exchanging power with the market.



a) Hourly profit



b) Hourly costs and profits

Fig. 9 comparison of the hourly revenues, costs and profits with and without the DR (in euro)

We have also investigated the effect of the electrical storages on the profit of the VPP. Without the presence of the electrical storages, the total profit for the VPP will be -516.8 euro, which is 1.3% less than the case with their presence. In fact, electrical storages enable the VPP to save energy during low purchase price periods and make it utilizable in those with high prices to decrease the cost of providing demand. The VPP can also sell the stored energy to the market to increase its profit. Therefore, the operation of the VPP with both the electrical storages and the DR program is beneficial.

5. CONCLUSION

A scheduling model to optimize the operation of the electrical and thermal resources of a large scale VPP in the presence of a DR program is proposed in this paper. The proposed model considers the revenue of the VPP from selling electricity to the energy market, and the cost of producing electrical and thermal energy as well as

purchasing electricity from the market. Simulation results show that the investigated DR program establishes a flexible hourly load curve that reaches a lower electrical demand for the VPP at peak hours. Therefore, the operation cost of the VPP decreases and its profit increases. Moreover, the inclusion of the storages enables the VPP to purchase less electrical energy from the market during high price periods since the excessive production of the internal resources or the purchase of electricity during low price periods can be saved and then be utilized at peak load hours. All in all, in terms of the operational cost, the presence of both the DR program and the storages is beneficial for the VPP and increases its profit.

Appendix A.

The equivalent linear inequalities for (8) are as follows:

$$1 + \frac{P_{int.R,t}}{M_1} \leq sale_{R,t} \leq \frac{P_{int.R,t}}{M_1} \quad (A.1)$$

$$C_{pcc.R,t} = \pi_{sp,t} E_{R,t} + \pi_{pp,t} F_{R,t} \quad (A.2)$$

$$P_{int.R,t} + (1 - sale_{R,t})M_1 \leq E_{R,t} \leq P_{int.R,t} - (1 - sale_{R,t})M_1 \quad (A.3)$$

$$0 \leq E_{R,t} \leq sale_{R,t} M_1 \quad (A.4)$$

$$P_{int.R,t} + sale_{R,t} M_1 \leq F_{R,t} \leq P_{int.R,t} - sale_{R,t} M_1 \quad (A.5)$$

$$-M_1(1 - sale_{R,t}) \leq F_{R,t} \leq 0 \quad (A.6)$$

where $sale_{R,t}$ is a binary variable which is 1 if the direction of $P_{int.R,t}$ is outward and 0 otherwise; M_1 is a large number; $E_{R,t}$ is the power output from Region R , and $F_{R,t}$ is the power input to region R .

The equivalent linear inequalities for Eq. (22) are as follows:

$$1 + \frac{P_{ES.R,t}}{M_2} \leq ZE_{R,t} \leq \frac{P_{ES.R,t}}{M_2} \quad (A.7)$$

$$P_{ES.R,t} + (1 - ZE_{R,t})M_2 \leq B_{R,t} \leq P_{ES.R,t} - (1 - ZE_{R,t})M_2 \quad (A.8)$$

$$0 \leq B_{R,t} \leq ZE_{R,t} P_{ES-disc.R} \quad (A.9)$$

$$P_{ES.R,t} + ZE_{R,t} M_2 \leq A_{R,t} \leq P_{ES.R,t} - ZE_{R,t} M_2 \quad (A.10)$$

$$-(1 - ZE_{R,t}) P_{ES-ch.R,t} \leq A_{R,t} \leq 0 \quad (A.11)$$

where $ZE_{R,t}$ is a binary variable which is 1 if the electrical storage in region R is charging at time t , and 0 otherwise. M_2 is a large number and $A_{R,t}$ and $B_{R,t}$ are the

charge and discharge power of the electrical storage in region R at time t , respectively.

The equivalent linear inequalities for Eq. (23) are:

$$1 + \frac{P_{TS.R,t}}{M_3} \leq ZT_{R,t} \leq \frac{P_{TS.R,t}}{M_3} \quad (A.12)$$

$$P_{TS.R,t} + (1 - ZT_{R,t})M_3 \leq D_{R,t} \leq P_{TS.R,t} - (1 - ZT_{R,t})M_3 \quad (A.13)$$

$$D_{R,t} \leq ZT_{R,t} P_{TS-ch.R} \quad (A.14)$$

$$P_{TS.R,t} + (1 - ZT_{R,t})M_3 \leq C_{R,t} \leq P_{TS.R,t} - (1 - ZT_{R,t})M_3 \quad (A.15)$$

$$-(1 - ZT_{R,t})P_{TS-disc.R,t} \leq C_{R,t} \leq 0 \quad (A.16)$$

where $ZT_{R,t}$ is a binary variable which is 1 if the thermal storage in region R is charging at time t , and 0 otherwise. M_3 is a large number; and $C_{R,t}$ and $D_{R,t}$ are the charge and discharge power of the thermal storage in region R at time t , respectively.

Appendix B.

The main and alternative load profiles of the customers are shown below:

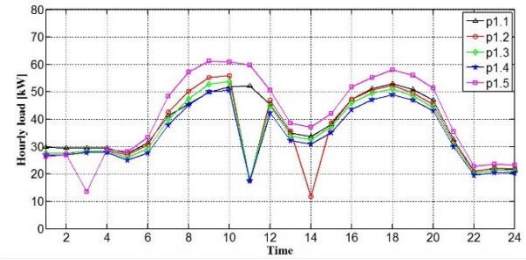


Fig. 10 The load profiles submitted by customer 1

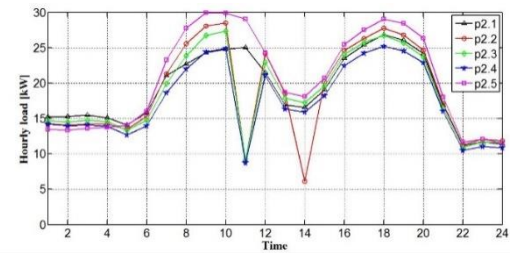


Fig. 11 The load profiles submitted by customer 2

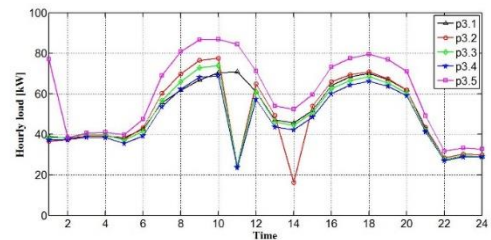


Fig. 12 The load profiles submitted by customer 3

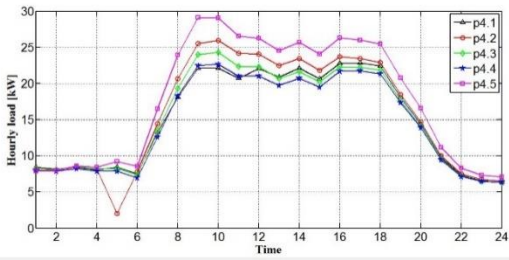


Fig. 13 The load profiles submitted by customer 4

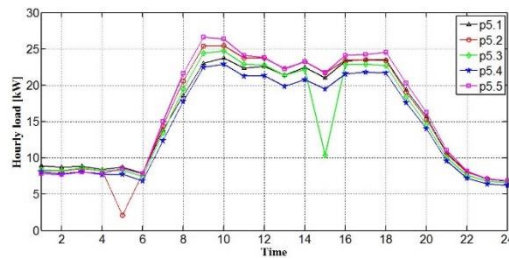


Fig. 14 The load profiles submitted by customer 5

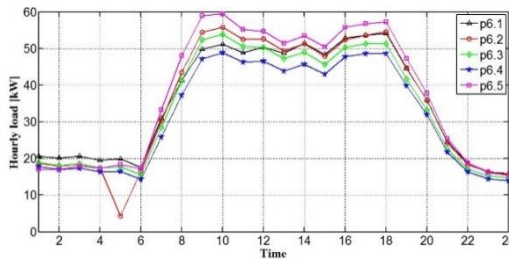


Fig. 15 The load profiles submitted by customer 6

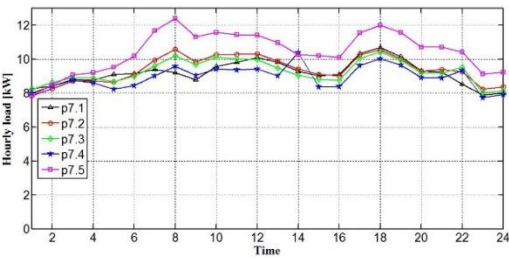


Fig. 16 The load profiles submitted by customer 7

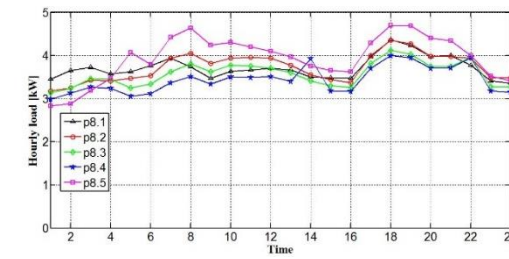


Fig. 17 The load profiles submitted by customer 8

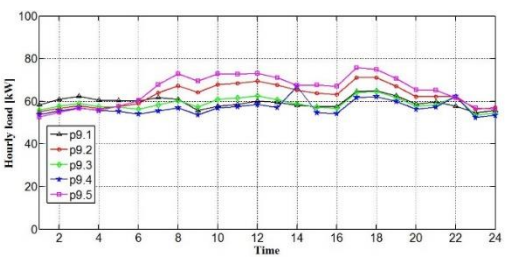


Fig. 18 The load profiles submitted by customer 9

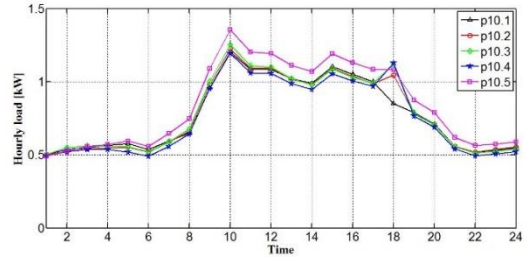


Fig. 19 The load profiles submitted by customer 10

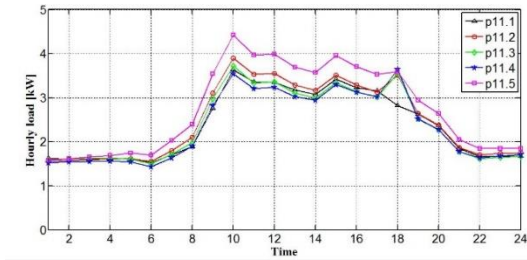


Fig. 20 The load profiles submitted by customer 11

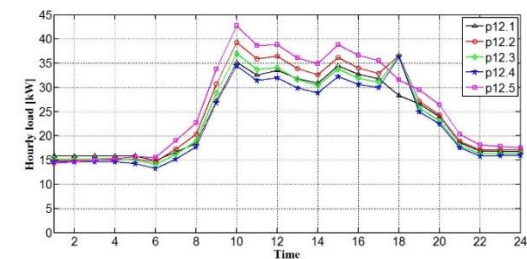


Fig. 21 The load profiles submitted by customer 12

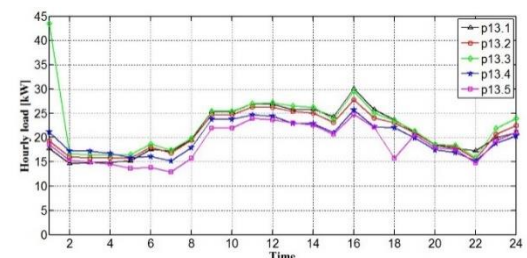


Fig. 22 The load profiles submitted by customer 13

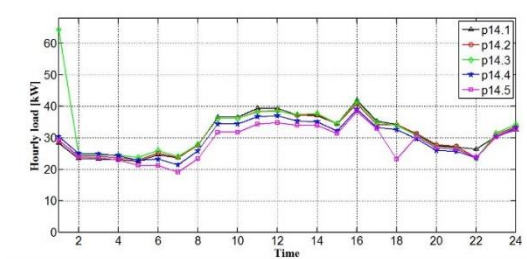


Fig. 23 The load profiles submitted by customer 14

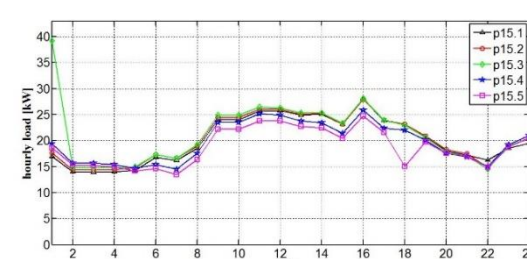


Fig. 24 The load profiles submitted by customer 15

REFERENCES

- [1] L. I. Dulău, M. Abrudean, and D. Bică, "Effects of Distributed Generation on Electric Power Systems," *Procedia Tech.*, vol. 12, pp. 681-686, 2014.
- [2] M. A. Tajeddini, A. Rahimi-Kian, and A. Soroudi, "Risk averse optimal operation of a virtual power plant using two stage stochastic programming," *Energy*, vol. 73, pp. 958-967, 2014.
- [3] S. R. Dabbagh and M. K. Sheikh-El-Eslami, "Risk-based profit allocation to DERs integrated with a virtual power plant using cooperative Game theory," *Electr. Power Syst. Res.*, vol. 121, pp. 368-378, 2015.
- [4] S. Pazouki, M. R. Haghifam, and S. Pazouki "Transition from fossil fuels power plants to ward virtual power plants of distribution networks," in Proc. of the EPDC, Karaj, Iran, 2016, pp. 82-86.
- [5] P. Asmus, "Micro grids, virtual power plants and our distributed energy future," *Electr. J.*, vol. 23, no. 8, pp. 72-82, 2010.
- [6] M. Peik-Herfeh, H. Seifi, and M. K. Sheikh-El-Eslami, "Decision making of a virtual power plant under uncertainties for bidding in a day-ahead market using point estimate method," *Electr. Power Energy Syst.*, vol. 44, no. 1, pp. 88-98, 2013.
- [7] H. Pandzic, J. M. Morales, A. J Conejo, and I. Kuzle, "Offering model for a virtual power plant based on stochastic programming," *App. Energy*, vol.105, pp. 282-292, 2013.
- [8] E. Mashhour and S. M. Moghaddas-Tafreshi, "Bidding strategy of virtual power plant for participating in energy and spinning reserve markets - part I: problem formulation," *IEEE Trans. Power Syst.*, vol. 26, no. 2, pp. 949-56, 2011.
- [9] E. Mashhour and S. M. Moghaddas-Tafreshi, "Bidding strategy of virtual power plant for participating in energy and spinning reserve markets: part II: numerical analysis," *IEEE Trans. Power Syst.*, vol. 26, no. 2, pp. 957-64, 2011.
- [10] P. Faria, J. Soares, Z. Vale, H. Morais, and T. Sousa, "Modified particle swarm optimization applied to integrated demand response and DG resources scheduling," *IEEE Trans. Smart Grid*, vol. 4, no. 1, pp. 606-616, 2013.
- [11] M. Giuntoli and D. Poli, "Optimal thermal and electrical scheduling of a large scale virtual power plant in the presence of energy storage," *IEEE Trans. Smart Grid*, vol. 4, no. 2, pp. 942-955, 2013.
- [12] A. GH. Zamani, A. Zakariazadeh, S. Jadid, and A. kazemi, "Stochastic operational scheduling of distributed energy resources in a large scale virtual power plant," *Int. J. Electr. Power Energy Syst.*, vol. 82, pp. 608-620, 2016.
- [13] A. Yousefi, T. T. Nguyen, H. Zareipour, and O. P. Malik, "Congestion management using demand response and FACTS devices," *Electr. Power Energy Syst.*, vol. 37, no. 1, pp. 78-85, 2012.
- [14] Federal Energy Regulatory Commission Staff, "Assessment of demand response and advanced metering," *FERC*, 2007.
- [15] N. Çiçek and H. Deliç, "Demand response management for smart grids with wind power," *IEEE Trans. Sust. Energy*, vol. 6, no. 2, pp. 625-634, 2015.
- [16] Q. Wang, J. Wang, and Y. Guan, "Stochastic unit commitment with uncertain demand response," *IEEE Trans. Power Syst.*, vol. 28, no. 1, pp. 562-563, 2013.
- [17] M. Fathi and H. Bevrani, "Adaptive energy consumption scheduling for connected micro grids under demand uncertainty," *IEEE Trans. Power Del.*, vol. 28, no. 3, pp. 1576-1583, 2013.
- [18] P. R. Thimmapuram and J. Kim, "Consumers' price elasticity of demand modeling with economic effects on electricity markets using an agent based model," *IEEE Trans. Smart Grid*, vol. 4, no. 1, pp. 390-397, 2013.
- [19] E. Dehnavi, H. Abdi, and F. Mohammadi, "Optimal emergency demand response program integrated with multi-objective dynamic economic emission dispatch problem", *J. Oper. Autom. Power Eng.*, vol. 4, no. 1, pp. 29-41, 2016.
- [20] H. Arasteh, M. S. Sepasian and V. Vahidinasab, "Toward a smart distribution system expansion planning by considering demand response resources," *J. Oper. Autom. Power Eng.*, vol. 3, no. 2, pp.116-130, 2015.
- [21] L. Bajracharyay, S. Awasthi, S. Chalise, T. M. Hansen, and R. Tonkoski, "Economic analysis of a data center virtual power plant participating in demand response," Proc. *Powe Energy Soc. General Meeting*, Boston, MA, USA, 2016, pp. 1-5.
- [22] H.T. Nguyen and L.B. Le, "Bidding strategy for virtual power plant with intraday demand response rxchange market using stochastic programming," Proc. *IEEE Int. Conf. Sustain. Energy Tech.*, Hanoi, Vietnam, 2016, pp. 96-101.
- [23] A. Mnatsakanyan and S. W. Kennedy, "A novel demand response model with an application for a virtual power plant," *IEEE Trans. Smart Grid*, vol. 6, no. 1, pp. 230-237, 2014.
- [24] Available at:
http://www.nyiso.com/public/markets_operations/market_data/graphs/index.jsp.